Towards an Infragravity Wave Climate for New South Wales

A.F. Nielsen[1], B. Williams[1], P.D. Treloar[2], C. Scraggs[2]
[1] Advisian WorleyParsons, North Sydney, NSW, Australia, Lex.Nielsen@Advisian.com
[2] Cardno, St Leonards, NSW, Australia

Abstract
Infragravity (IG) waves may cause dangerous ranging of moored ships having resonant natural frequencies of oscillation, which can be exacerbated in harbour basins having resonant IG length scales. To aid navigation the Port Kembla Port Corporation established two bottom-mounted Acoustic Doppler Current Meters (ADCPs) with pressure sensors offshore of the port entrance to monitor swell waves and currents. From long time series of high frequency surface displacement data it has been possible to elicit nearshore IG wave events along with their concomitant swell wave characteristics. Having concomitant Waverider buoy data offshore it has been possible to develop relationships between the nearshore IG wave data and the deep water swell wave characteristics based on theoretical analysis calibrated with field data. From those relationships an IG wave climate has been developed from the long term Waverider buoy data. This paper presents a methodology for and the results from developing, theoretically and empirically, an IG wave climate for the NSW coast based on field data. As Fourier transformation does not describe shallow water wave spectra correctly, an alternative method of describing shallow water IG wave spectra is presented.

Keywords: infragravity, long wave, climate, field data.

1. Introduction

Generally, infragravity (IG) waves (or long waves) have periods ranging from 30 s to 300 s with wave heights of decimetres, although far infragravity waves, such as tsunamis or shelf waves, have much longer periods and greater wave heights.

Some IG waves are bound to swell and can be released as free waves through swell waves breaking on a beach. While IG waves can be found everywhere in the ocean, they are ubiquitous near beaches. The IG waves that are the subject of this study comprise those bound to swell sets propagating onshore and free waves propagating offshore but refracting back onshore, resulting in complex IG wave transformation processes.

Field data on IG waves are scarce as they can be measured only with fixed instruments, such as submerged pressure sensors or capacitance-type wave probes, recording nearly continuously. By happenstance, the Port Kembla Port Corporation established bottom-mounted ADCPs with pressure sensors offshore of the port that monitor swell waves and currents to assist navigation. These instruments capture IG waves also.

From long time-series of high frequency surface displacement data it has been possible to elicit nearshore IG wave events and their concomitant forcing swell wave characteristics. These data have allowed the development of relationships between the nearshore swell and IG wave characteristics and those of the deep water swell waves. This paper presents such data and a methodology that may be relevant to the assessment of infragravity wave processes along the New South Wales coast.

2. Field Data

2.1 Nearshore Data

The Port Authority of NSW operates real-time wave and current meter stations at a location about 600 m north of the entrance to Port Kembla Harbour. These instruments (RDI 300 kHz Sentinel ADCP with waves) record waves and currents in a depth of about 19 m with a water level pressure sensor located about 0.5 m above the seabed. The current data is recorded in about 15 m depth using 0.5 m bins. The first ADCP was installed in 2007. However, the raw data was not archived routinely prior to 2011.

2.2 Offshore Data

Since 1974 Manly Hydraulics Laboratory has collected wave data at Port Kembla with a Datawell Waverider buoy that has been moored in ~80 m water depth ~10 km offshore [3].

2.3 Relationships Between ADCP and Waverider Swell Wave Data

Relationships between the deep water Waverider and nearshore ADCP *significant* wave heights and zero-crossing wave periods were developed empirically (Figure 1) to generate deep water wave conditions for some measured IG wave data where Waverider data were missing. The nearshore wave height refraction coefficient was 0.80, R^2=0.34, the scatter probably due to variations in offshore wave direction (with 77% of storm waves coming from SE to S and 23% from ENE to ESE) as well as the random nature of the natural processes. For the zero-crossing wave period the coefficient was 1.22, R^2=0.34, being higher than 1.0 because the ADCP samples wave period at a depth that filters out the higher frequency wave energies.

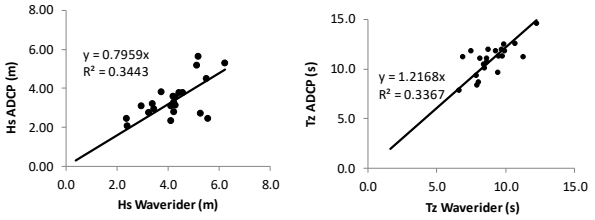

Figure 1 Relationships between the deep water Waverider and nearshore ADCP *significant* wave heights (left) and zero-crossing wave periods (right)

2.4 Data Selected for IG Wave Analysis

Previous studies indicated that IG waves were likely to occur when the parameter Hs*Tz was larger than 20 [9]. The archived, processed 2011-2017 wave dataset was interrogated to select storms with Hs*Tz above 20. For these data, this resulted in the selection of 23 storms for which raw data was found. Of these the seven most severe storms were selected for IG wave analysis presented herein.

Three-dimensional polar spectral plots undertaken on the peaks (4,096 s) of each of these storms gave data for 25 IG waves with energies of various intensities, peaking at various frequencies and coming from various directions; that is, each hourly record produced simultaneous signatures of up to several IG waves. The wave height for each IG wave was determined from the total IG wave height, given by the spectral analysis, being the square root of the sum of the individual IG wave heights squared.

The data gave an average significant IG wave height of 0.18 m and a maximum significant IG height of 0.29 m for twenty-five IG waves. The average offshore significant swell wave height was 4.9 m, ranging from 3.5 m to 6.2 m, with an average T_z of 9.4 s, ranging from 8.5 s to 11.2 s.

These data were combined with the dataset that had been obtained from the analysis of storm wave data recorded on 1st to 5th January 2008 [9]. For those data, twenty IG waves, the average significant IG wave height was 0.12 m and a maximum significant IG height was 0.22 m. The average offshore significant wave height was 3.2 m, ranging from 2.1 m to 3.6 m, with an average T_z of 8.3 s ranging from 7.1 s to 9.3 s.

The reduced data are appended.

3. Data Analyses

3.1 Spectral Analysis

The wave heights and periods of the IG waves of interest herein have been estimated from time series of pressure fluctuations (time domain). Commonly, such time-domain data have been analysed to obtain wave energy spectra (frequency domain) using a Fourier transformation, which transforms a random wave train into a series of sinusoids of various amplitudes and periods (frequencies). This gives a measure of the amount of wave energy, from which a characteristic wave height may be derived, and the frequency, hence wave period, around which the energy peaks; that is, the *significant* wave height and peak period of the IG wave and the distribution of its energy over the frequency range.

The Fourier transformation is used commonly on Waverider data that capture swell waves in deep water (relative to the swell wavelength). However, data for IG waves can be captured only by pressure transducers or capacitance probes in relatively shallow nearshore water depths (5-20 m say). Hence, the IG wave is recorded in relatively shallow water and, as such, is not sinusoidal. Carrying out Fourier transformation on a shallow water wave will result in false spectral energy spikes at frequencies higher than the peak frequency of the carrier wave as higher frequency sinusoids are required to describe a shallow water wave shape [10].

For example, a regular shallow water wave of period T = 200 s, wave height H = 0.58 m in a water depth of 10 m is described by Stream Function theory [2] and is presented in Figure 2. A Fourier transform energy spectrum of this wave form is in Figure 3.

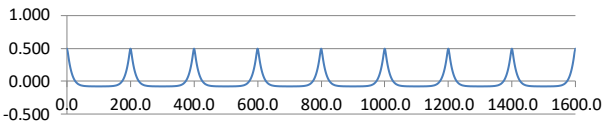

Figure 2 Regular shallow water wave of T = 200 s, H = 0.58 m in a water depth of 10 m as described by Stream Function theory [2] indicating the severe distortion that occurs to a regular deep-water sinusoid wave in shallow water.

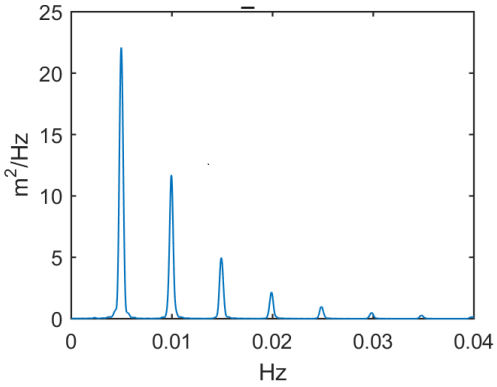

Figure 3 Wave energy spectrum determined by a Fourier transformation of the regular shallow water wave form in Figure 2. This plot shows several energy peaks at frequencies that are harmonics of the carrier frequency 0.005 Hz. There are no wave forms at these frequencies apparent in Figure 2.

The energy spectrum in Figure 3 shows the peak energy at a frequency of 0.005 Hz (period 200 s) with subsequent energy spikes at 0.01 Hz (100 s),

0.015 Hz (66.6 s), 0.02 Hz (50 s) . . . The higher frequency energy spikes are not real as there are no wave forms of those frequencies in the regular wave train in Figure 2 that was analysed. They are harmonics of the carrier frequency that were created by the Fourier transformation to describe with sinusoids the distorted shape of a shallow water wave.

A Fourier analysis was undertaken on the IG wave data derived during the peak of the most severe storm in the field data, recorded on 21 April 2015. The directional spectral plot in Figure 4 shows three spectral peaks at frequencies (periods) of 0.0055 Hz (180 s), 0.0110 Hz (90 s) and 0.0165 Hz (60 s), each directed westward onshore. The two higher frequency peaks appear to be the first and second harmonic of the carrier frequency.

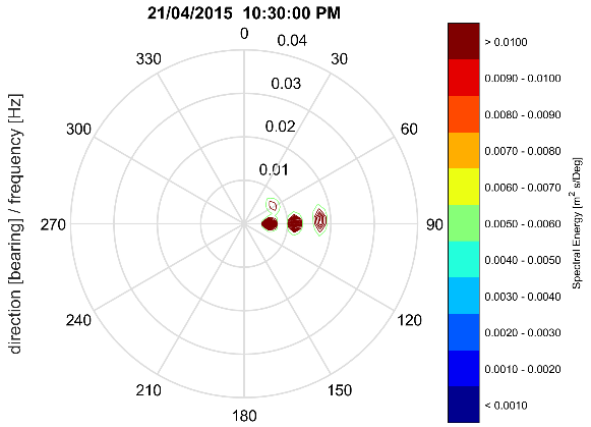

Figure 4 Directional Fourier spectral plot for the peak of the severe storm of 21 April 2015. This plot shows three spectral peaks at 180 s, 90 s and 60 s all directed from the east.

As Fourier transformation from the time to frequency domain allocates incorrectly shallow water wave energy to frequencies that are higher than the carrier frequency, appropriate spectra can be developed by filtering the time domain data into frequency bands and spectral shapes can be derived from the variances of each frequency band, as shown in Figure 5 for the storm peak of 21 April 2015. There may be other appropriate techniques.

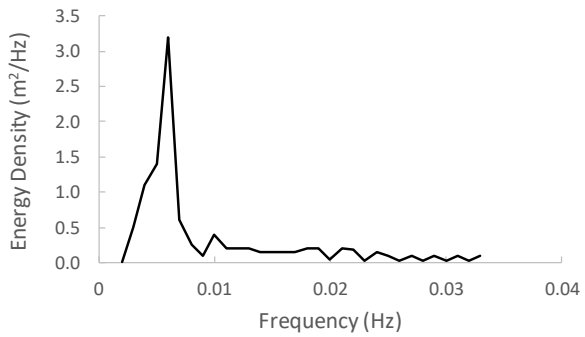

Figure 5 A variance IG wave energy spectrum derived for the storm peak of 21 April 2015.

The variance spectral plot in Figure 5 shows no peaks at frequencies higher than the carrier frequency, which were evident in the spectral plot derived from the Fourier transformation in Figure 4. The variance spectral shape can be factored to schematise the total wave energy that has been derived from a Fourier transform.

3.2 IG Wave Directions

IG wave directions were derived from polar spectral plots of the seven most severe storms in the record from 2011 to 2017, as exemplified in Figure 6, and from 10 polar spectral plots from the 5-day storm in 2008. Twenty-five waves were identified from the 2011 to 2017 dataset with twenty waves from the 2008 study. Their directional distribution ranged widely around the compass (Figure 7). IG waves heading onshore, being directed southwest to west, comprised 44% of the total with the remaining 56% directed variously from north through west to south assumed to be free IG waves as swell does not come from those directions at the ADCP site.

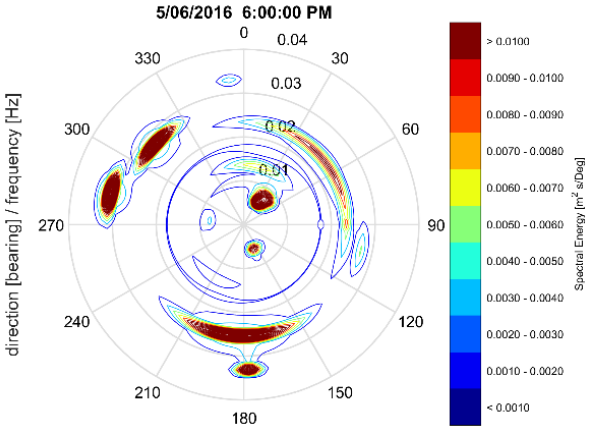

Figure 6 Directional Fourier spectral plot at the peak of the severe storm of June 2016 showing the capture of several IG wave forms with some headed south-westerly onshore coming from the NE quadrant and several directed offshore in northerly to south-easterly directions

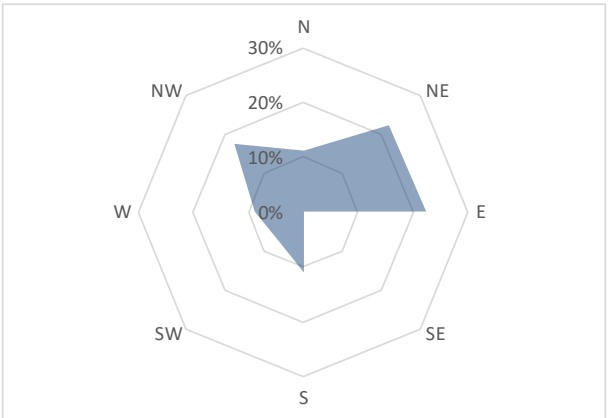

Figure 7 Directional distribution of the IG waves identified in the polar spectra of the peaks of the seven most severe storms between 2011 and 2017 (25 waves) and from the storm in June 2008 (20 waves).

3.3 IG Wave Periods

IG wave peak periods derived from the polar spectral plots ranged from around 30 s to 200 s, with most (26%) in the range 40-70 s (Figure 8).

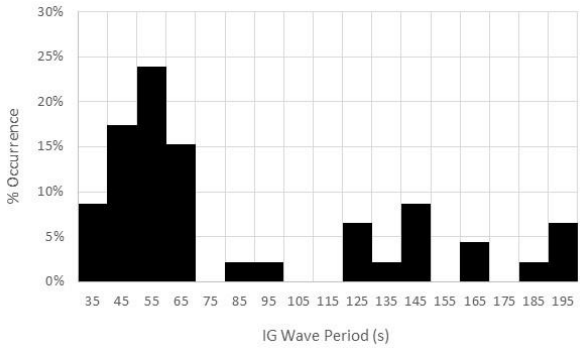

Figure 8 The distribution of spectral peak periods from forty-five IG waves derived from the polar spectral plots

4. Theory

The relationship between the nearshore IG wave height (H_{IG}) and deep water swell wave parameters (H, T) is given by an empirical expression:

$$H_{IG} = k\frac{H^{\alpha}T^{\beta}}{d^{\gamma}} \qquad (1)$$

where d is the water depth and k, α, β, γ are site-specific empirical parameters [5].

The main source of infragravity waves nearshore is associated with wave grouping; set down beneath wave groups generating the infragravity wave height [1]. Maximum wave set down, S_b, occurs at the point of wave break, which is given by [8]:

$$S_b = \left(\frac{g}{d_b}\right)^{0.5}\frac{H_b^2 T}{64\pi d_b} \qquad (2)$$

For the storm conditions considered herein ($H_{mo} \approx 5$ m, $T_p \approx 12$ s) and a beach slope ≈ 1:50, deep water wave steepness is around 0.0034, giving a breaker height index of $H_b/H_o = 1.20$ [8; Fig 2-72] and a breaker depth index of $d_b/H_b = 1.15$ [8; Fig 2-73]. Given the relationship $T_s/T_z = 1.38$ [4], Equation *(2)* reduces to:

$$S_b = 0.003T_z(gH_s)^{0.5} \qquad (3)$$

5. Results

5.1 Relationship between IG Wave Height and Swell Wave Characteristics

Relationships in the form of Equation (3) between the nearshore IG significant wave height and offshore wave characteristics at Port Kembla for onshore-directed, offshore-directed and all IG waves are presented in Figure 9. The slopes of the lines of best fit ranged from 0.0023 to 0.0030 with an overall average value of 0.0028, which approximated closely the theoretical value of 0.0030 as derived in Equation (3). For design, a non-exceedance relationship is presented, employing a "background" value for IG wave height of 0.08 m, assuming IG wave energy always is present, as expressed in Equation (4).

$$S_b = 0.003T_z(gH_s)^{0.5} + 0.08\,m \qquad (4)$$

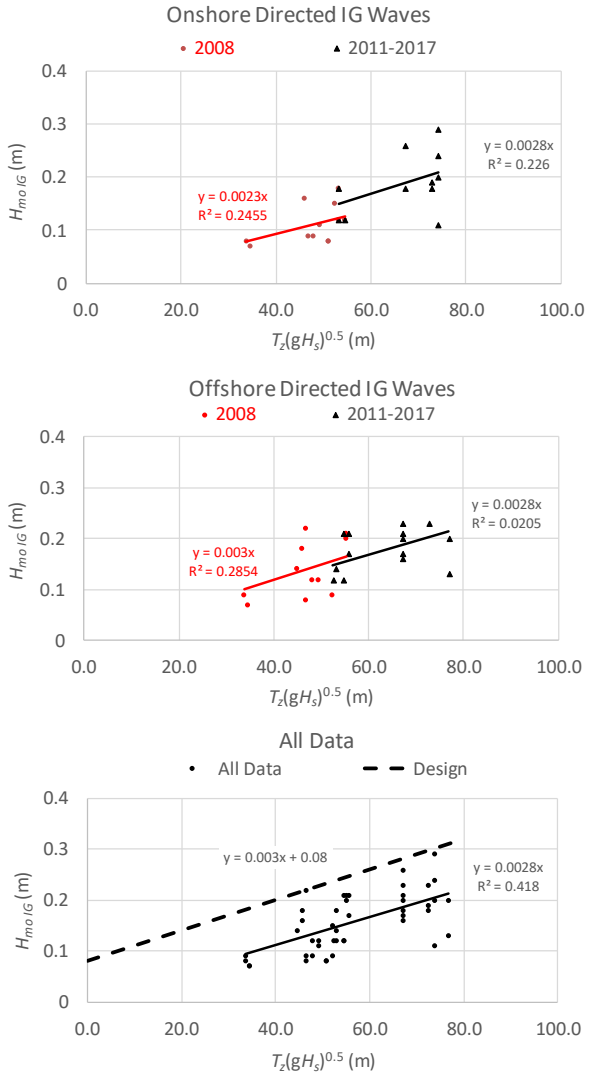

Figure 9 Relationships between nearshore IG wave height and offshore wave characteristics at Port Kembla for onshore-directed waves (top), offshore-directed waves (centre) and for all IG waves (bottom). For design, a non-exceedance relationship is presented (bottom)

5.2 IG Wave Climate

IG wave height occurrences were derived from long-term data of one-hour duration storm swell wave height occurrences determined from the offshore Waverider data collected at Port Kembla using Equation (4) and the following relationship between significant wave height and zero-crossing wave period derived from the Port Kembla Waverider data (Figure 10):

$$T_z = 0.9H_s + 4.8 \qquad (5)$$

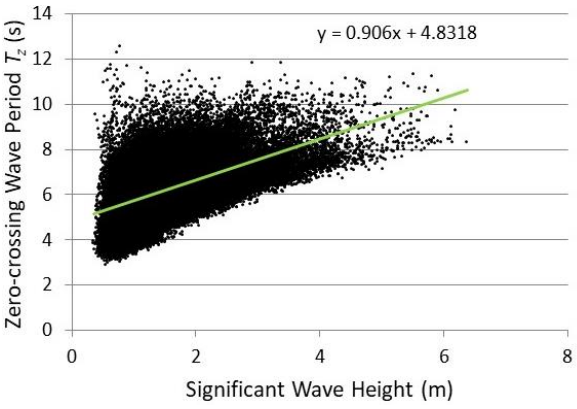

Figure 10 Relationship between T_z and H_s at Port Kembla based on data from 2007-2018 [3]

which relationship agrees closely with some four years of data from the Newcastle, Botany Bay and Jervis Bay Waverider buoys, for which $H_{s\ mean}$ = 1.36 m and $T_{z\ mean}$ = 5.84 [4]. The result is in Figure 11, noting significant extrapolation beyond the meagre data set.

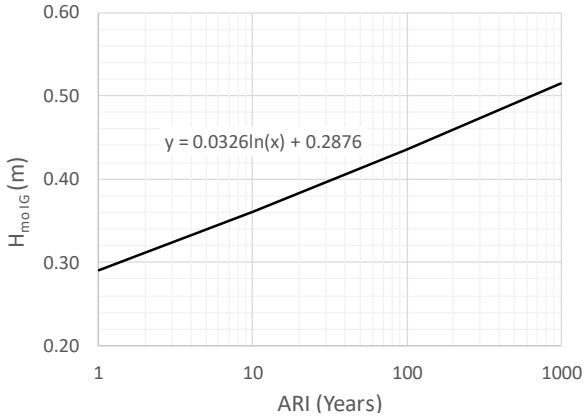

Figure 11 Derived significant nearshore IG wave height occurrences at Port Kembla, NSW

As wave height exceedances are similar along the NSW coast between Byron Bay and Eden [6], the relationship in Figure 11 could be used as a first approximation for a nearshore IG wave climate along the NSW coast, notwithstanding that it is based on a meagre field data set.

6. Summary and Conclusions

The simultaneous occurrence nearshore of onshore directed and offshore directed infragravity waves is ubiquitous adjacent to beaches. To sample and differentiate the simultaneous occurrence of several IG waves, field data necessarily must comprise *P, U, V* measurements, which can be obtained only by seabed mounted ADCP-type instruments equipped with pressure sensors. Such data enable the identification of IG waves through the generation of 3-D polar spectral plots by Fourier transformation. An analysis of such data sets has enabled a first approximation of a nearshore IG wave climate for the NSW coast.

The investigation of such phenomena at any specific location is informed, typically, by Boussinesq long wave transformation modelling. However, Fourier transformation is not applicable for shallow water waves as it may generate false energy peaks at frequencies that are higher than that of the carrier wave. Appropriate IG wave energy spectra for numerical modelling may be generated by filtering the sea surface displacement signal into discrete frequency bands and defining the distribution of the wave energy with the variance of each frequency band. The resulting spectral shape can be factored to yield the total wave energy obtained from a Fourier transformation.

7. Acknowledgements

Nearshore ADCP data were provided by the Port Authority of New South Wales. Waverider buoy data is funded by the NSW Office of Environment and Heritage and provided by Manly Hydraulics Laboratory. The authors are responsible for the reduction, analysis and presentation of these data.

8. References

[1] BS 6349-1 (2000). Maritime Structures - Part 1: Code of Practice for General Criteria, British Standards Institution.

[2] Dean, R.G. (1965). Stream function representation of nonlinear ocean waves, *Jnl. Geophys. Res*., Vol 70, Issue 18, September 1965.

[3] http://mhl.nsw.gov.au/data/realtime/wave/docs/PortKembla.pdf

[4] Lawson, N.V., A.D. McCowan and P.D. Treloar (1987). Inter-Relationships between wave periods for the NSW Australia Coast, 8th Aust. Conf. on Coastal and Ocean Engg., Launceston, IEAust., pp 424-429.

[5] Lopez, M. and G. Iglesias (2013). Artificial intelligence for estimating infragravity energy in a harbour, *Ocean Engineering,* 57, pp 56-63.

[6] Lord, D.B. and M. Kulmar (2000). The 1974 storms revisited: 25 years' experience in ocean wave measurement along the south-east Australian coast, *Coastal Engineering 2000*, ASCE, pp 559-572.

[7] Nielsen, A.F., J. Opkar and T. Pinzone (2010). *Port Kembla Outer Harbour Development Environmental Assessment, Appendix F Coastal Hydrodynamic Processes*, Report prepared by AECOM Australia in conjunction with Cardno Lawson Treloar and OMC International for Port Kembla Port Corporation, January 2010, 16 pp.

[8] SPM (1984). *Shore Protection Manual*, Coastal Engineering Research Centre, US Army Corps of Engineers.

[9] Treloar, P.D. (2008). *Port Kembla Outer Harbour Masterplan. Numerical Long Wave Modelling*, Cardno Lawson Treloar Report (LJ2689/R2439) prepared for Maunsell Australia (in [7]).

[10] Young, I. (pers. comm.). University of Melbourne, Nielsen/Young Coasts & Ports 2009; email 2019.

Appendix – Reduced Field Data

Date Time	Nearshore Infragravity Wave Data			*Offshore Wave Data*		
	$H_{mo\,IG}$ (m)	$T_{p\,IG}$ (s)	Direction (from) °TN	H_s (m)	T_z (s)	Direction (from) °TN
1/01/2008 13:00	0.08	200	45	2.3	7.1	112
1/01/2008 13:00	0.09	63	315	2.3	7.1	112
3/01/2008 17:00	0.07	59	45	2.1	7.6	112
3/01/2008 17:00	0.07	63	225	2.1	7.6	112
4/01/2008 22:00	0.14	63	315	3.2	8.0	112
5/01/2008 0:00	0.18	125	248	3.2	8.2	112
5/01/2008 0:00	0.16	125	68	3.2	8.2	112
5/01/2008 1:00	0.08	50	45	3.5	8.7	112
5/01/2008 1:00	0.08	125	90	3.5	8.7	112
5/01/2008 2:00	0.09	63	90	3.3	8.2	112
5/01/2008 2:00	0.08	63	315	3.3	8.2	112
5/01/2008 2:00	0.22	53	0	3.3	8.2	112
5/01/2008 3:00	0.11	53	45	3.5	8.4	112
5/01/2008 3:00	0.12	63	315	3.5	8.4	112
5/01/2008 4:00	0.09	143	45	3.4	8.3	112
5/01/2008 4:00	0.12	56	315	3.4	8.3	112
5/01/2008 5:00	0.15	148	45	3.6	8.8	112
5/01/2008 5:00	0.09	53	270	3.6	8.8	112
5/01/2008 6:00	0.21	200	225	3.6	9.3	112
5/01/2008 6:00	0.20	200	315	3.6	9.3	112
6/06/2012 7:30	0.12	53	90	4.2	8.5	Not available
6/06/2012 7:30	0.12	34	0	4.2	8.5	Not available
6/06/2012 7:30	0.21	83	320	4.2	8.5	Not available
6/06/2012 7:30	0.12	43	190	4.2	8.5	Not available
1/08/2012 6:00	0.18	143	80	3.8	8.7	142
1/08/2012 6:00	0.12	53	90	3.8	8.7	142
1/08/2012 6:00	0.14	40	10	3.8	8.7	142
21/04/2015 22:30	0.24	182	90	6.2	9.5	135
21/04/2015 22:30	0.11	133	60	6.2	9.5	135
21/04/2015 22:30	0.20	91	90	6.2	9.5	135
21/04/2015 22:30	0.29	61	85	6.2	9.5	135
25/05/2016 10:30	0.20	40	0	4.8	11.2	155
25/05/2016 10:30	0.13	50	290	4.8	11.2	155
5/06/2016 18:00	0.18	42	50	5.2	9.4	90
5/06/2016 18:00	0.26	143	40	5.2	9.4	90
5/06/2016 18:00	0.17	36	315	5.2	9.4	90
5/06/2016 18:00	0.21	31	285	5.2	9.4	90
5/06/2016 18:00	0.20	167	160	5.2	9.4	90
5/06/2016 18:00	0.23	40	180	5.2	9.4	90
5/06/2016 18:00	0.16	30	180	5.2	9.4	90
24/10/2016 10:30	0.21	40	0	3.5	9.5	145
24/10/2016 10:30	0.17	50	290	3.5	9.5	145
20/08/2017 3:00	0.19	53	90	5.5	9.9	149
20/08/2017 3:00	0.18	40	70	5.5	9.9	149
20/08/2017 3:00	0.23	167	180	5.5	9.9	149

Note: All IG data are based on Fourier transformation polar spectral plots. Possible harmonics have been interpreted as individual IG waves.